Supplemental materials to the manuscript "Self-diffusion of spherocylindrical particles flowing under non-uniform shear rate"

I. Analysis for the yy- and yz-component of the diffusion tensor

In the main document of the manuscript, our analysis focuses on the z-component of the diffusivity tensor. Here, it is extended to two additional components D_{yy} and D_{yz}. The components related to the advection direction, x, have been excluded, due to the non-affine displacements could not simply be isolated by subtracting the displacement that results from integrating the individual particle velocities. Here, we could argue that the non-constant shear rate introduces a Taylor dispersion that we were not able to eliminate using the mentioned procedure.

As a first step, we examine the particles' mean squared displacements in the *yy-* and *yz-directions* (MSD_{yy} and MSD_{yz}) as a function of the time-lag τ. The expressions that describe MSD_{yy} and MSD_{yz} are respectively,

$$\mathrm{MSD}_{yy}(\tau) = 1/N_k \sum_{i}^{N_k} (y_i(\tau+t) - y_i(t))^2$$

$$\mathrm{MSD}_{yz}(\tau) = 1/N_k \sum_{i}^{N_k} (y_i(\tau+t) - y_i(t))(z_i(\tau+t) - z_i(t))$$

averaged over specific particle ensembles with N_k particles. The rest of the procedure is carried out as in the manuscript. That means the system is split in vertical direction into 20 blocks of width $\Delta H = L$ in terms of the particle's longest size L. Moreover, the particles are tracked for a total time elapsed of $\tau_T = 120\,s$ with a resolution $\delta_\tau = 0.05\,s$.

Fig. 1 shows examples for both a,c) $\mathrm{MSD}_{yy}(\tau)$ and b,d) $\mathrm{MSD}_{yz}(\tau)$ outcomes (in $\log - \log$ scale) for a subset of the sections labeled with H representing the region height $z = H$. In addition, the same data but using linear scale are displayed in the insets. The results correspond to the systems a,b) aspect ratio $\xi = 1.3$ and inclination $\alpha = 27°$ and c,d) aspect ratio $\xi = 2.5$ and inclination $\alpha = 30°$. As a guide to the eye, the graphs include continuous lines representing power-law functions with exponent 2 and 1 which stand for the ballistic and diffusive limit, respectively. Similarly to the diffusivity in the z direction, MSD curves change their behavior close to $\tau = 1\,s$. In detail, for $\tau < 1\,s$, the movement of the particles is ballistic; however, although there is reduction of the slopes, the movement remains superdiffusive for $\tau > 1\,s$. This result is more noticeable in the Fig. 1a) and differs from the obtained ones in the *z-direction*. For this reason, in these cases, we expect *a priori* no well-defined diffusivity values.

In any case, Fig. 2a and Fig. 2b exemplify the profiles of $D_{yy}(z)$ and $\dot{\gamma}(z)$ (and $D_{yz}(z)$ and $\dot{\gamma}(z)$) normalized by the maximum diffusion coefficient D_{max} and the maximum shear rate $\dot{\gamma}_{max}$ for $\xi = 1.3$ and $\xi = 2.5$, respectively. In both cases, we obtain that local diffusivity values do not correlate with the local shear rate values. Consequently, the simple scaling relation $D \sim d^2\dot{\gamma}$ does not seem to be a good choice.

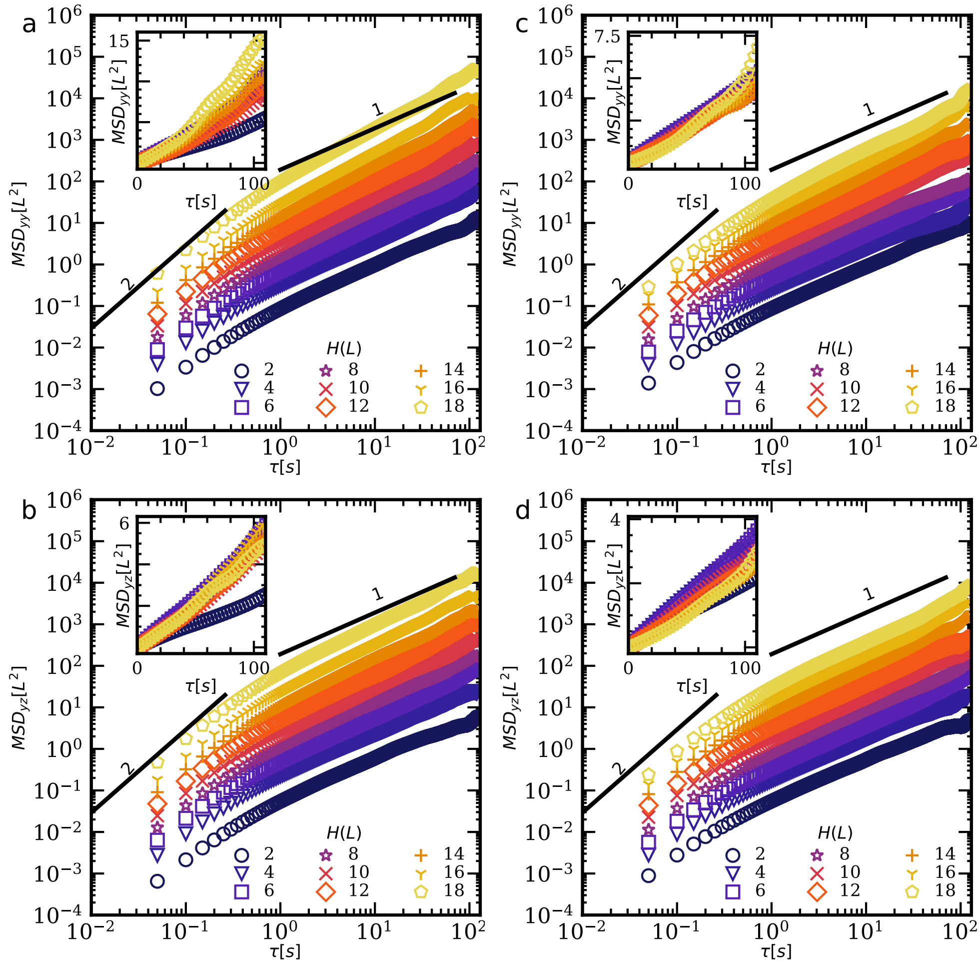

FIG. 1: The mean squared displacements (MSD) vs. τ for the cases a,b) $\xi = 1.3$, $\alpha = 27°$ and c,d) $\xi = 2.5$, $\alpha = 30°$ (both in log-log scales) in the a,c) yy- and b,d) yz-direction. Each curve represents the MSD calculated for each block of base equivalent to the system and width L whereas lines show the powers 1 and 2. In both cases, the inset shows the same but on linear scale.

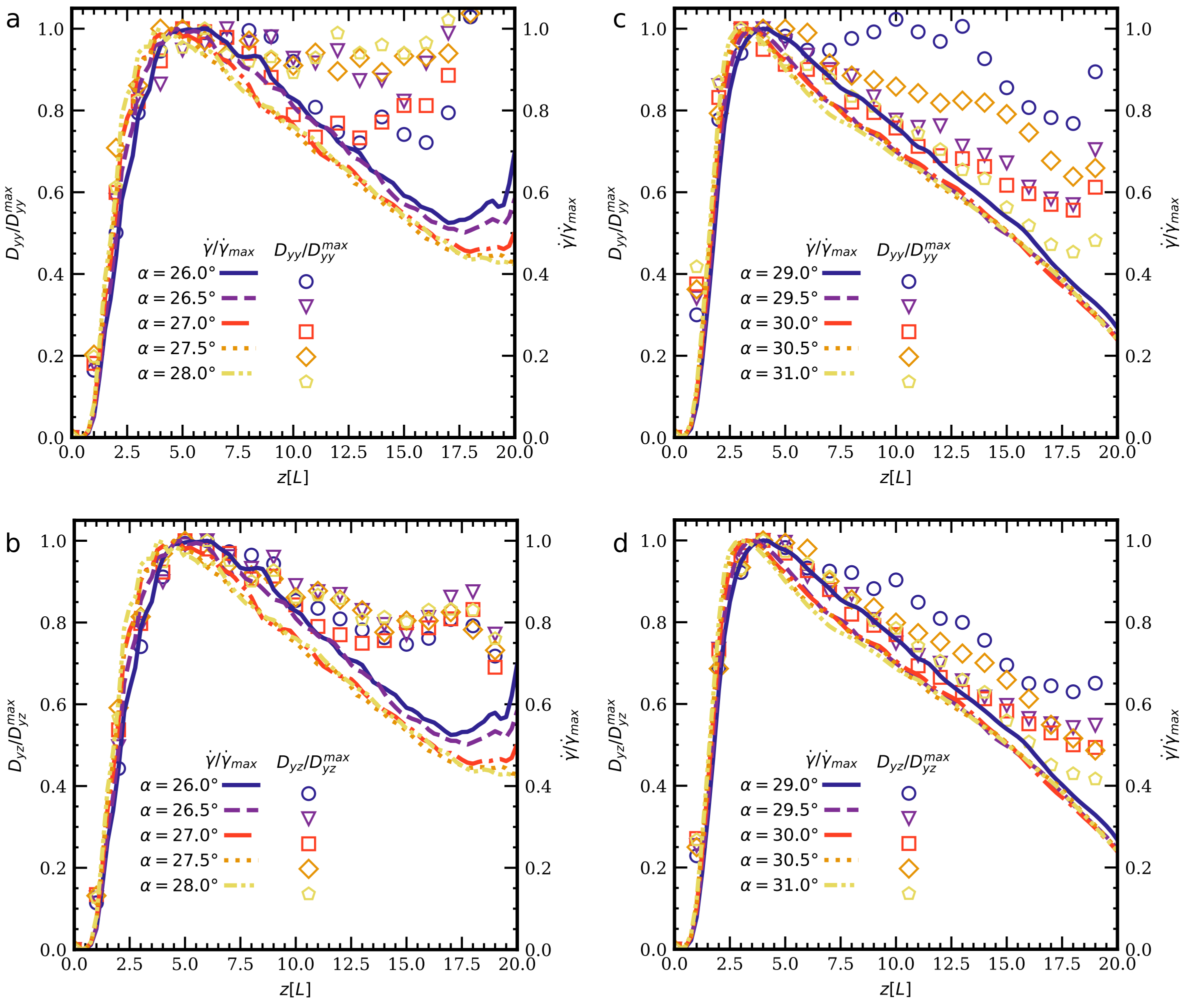

FIG. 2: Plots of a) D_{yy}/D_{yy}^{max}, b) D_{yz}/D_{yz}^{max} (markers) and $\dot{\gamma}/\dot{\gamma}_{max}$ (curves) against the height z for $\xi = 1.3$ and several inclinations, $\alpha = [26.0, 26.5, 27.0, 27.5, 28.0]^\circ$. c) and d) respectively display the same quantities but $\xi = 2.5$ and $\alpha = [29.0, 29.5, 29.0, 29.5, 30.0]^\circ$